Ring Closure Reaction Dynamics of Diarylethene Derivatives in Solution

Sangdeok Shim,† Intae Eom, and Taiha Joo*

Department of Chemistry, Pohang University of Science and Technology, Pohang 790-784, Korea

Eunkyoung Kim*

Department of Chemical Engineering, Yonsei University, Seoul 120-749, Korea

Kwang S. Kim

Center for Superfunctional Materials and Department of Chemistry, Pohang University of Science and Technology, Pohang 790-784, Korea

Received: February 25, 2007; In Final Form: May 24, 2007

Photochromic ring closure reaction dynamics of 1,2-bis(2-methylbenzo[*b*]thiophen-3-yl)hexafluoro cyclopentene and its derivatives in solution has been studied by femtosecond time-resolved fluorescence. Time-resolved spontaneous fluorescence of the open isomer reveals a fast component of around 1 ps and a slow component on the order of 100 ps. Fluorescence time profiles, reaction quantum yields, and relative populations of the parallel (C_s symmetry) and antiparallel (C_2 symmetry) conformations indicate that both time components are attributable mostly to the C_2 conformer that undergoes the ring closure reaction. The fast component is assigned to the direct ring closure reaction, and the slow component is assigned to the reaction through conformation change. Time constants of the slow component for the derivatives are inversely proportional to the reaction quantum yields, suggesting that the rate of the conformational dynamics is comparable to the rate of other population relaxation processes. The relative amplitude and exact time constant of the fast component depend on the detection wavelength displaying a higher relative amplitude with shorter time constant at longer wavelengths. The results allow us to propose a conformational inhomogeneity model, in which a broad distribution of conformations of the open isomers in the ground state is projected into two minima in the excited electronic potential surface to lead to the slow and the fast reaction pathways.

Introduction

Diarylethene derivatives have received much attention recently because of their potential application to various optoelectronic devices such as optical memories, optical switches, and display.[1,2] Diarylethene derivatives, especially with heterocyclic aryl groups, show excellent thermal stability and fatigue resistance that are indispensable for practical applications.[3−8] An additional requirement for the application is the fast reaction rate, which leads to high reaction quantum yield and high efficiency in optoelectronic devices. The high photochromic reaction quantum yield also reduces undesirable side reactions to give better fatigue resistance. Therefore, the study on the dynamics of the photochromic reactions provides valuable information for the design of the photochromic materials with improved optoelectronic properties.

A diarylethene molecule exists mostly as an open isomer after synthesis and is nearly colorless. Upon UV irradiation, the open isomer undergoes ring closure reaction, as shown in Scheme 1, whereas the ring opening reaction of the closed isomer can be initiated by visible light.[1] As shown in Figure 1, the closed isomer shows a new absorption band in the visible region due to the π-electron delocalization. The electrocyclic ring closure and ring opening reactions obey the Woodward−Hoffmann rule[9] based on the π-orbital symmetries of hexatriene, the basic framework of the diarylethene derivatives. According to the correlation diagram of the six π-electron electrocyclic reaction, the interconversion between the open and closed isomers is forbidden in the ground state whereas the two may convert by photoexcitation in the conrotatory mode.[10]

SCHEME 1: Chemical Structures of the Open and Closed Isomers of 1,2-Bis(2-methylbenzo[*b*]thiophen-3-yl)hexafluorocyclopentene (BTF6) and Its Derivatives[a]

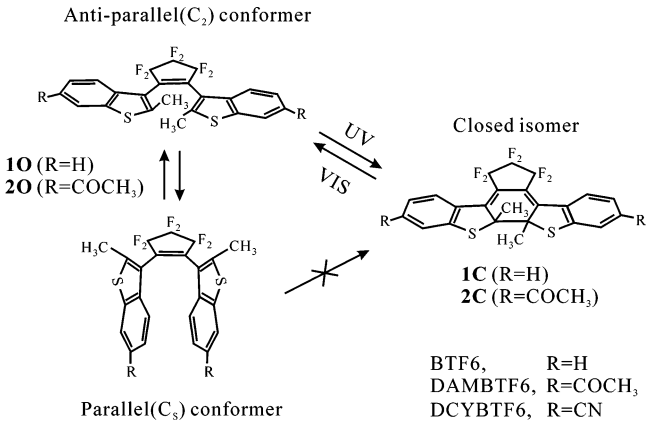

[a] UV and visible lights induce ring closure and opening reactions, respectively. It is also shown that the antiparallel (C_2) conformer can undergo the ring closure reaction, whereas the parallel (C_s) conformer cannot.

† Present address: Department of Chemistry, University of California, Berkeley, CA 94720.

10.1021/jp0715528 CCC: $37.00
Published on Web 08/28/2007

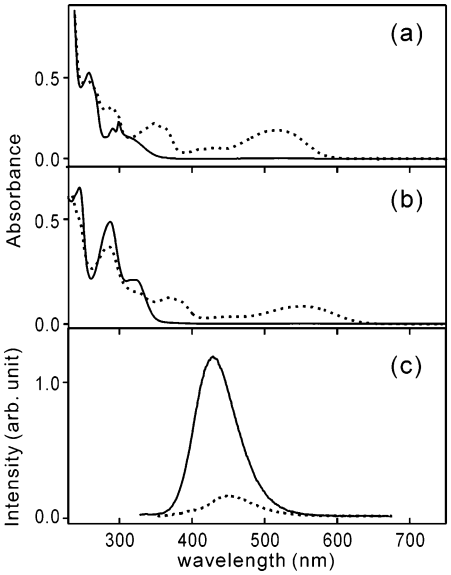

Figure 1. Absorption spectra of the open isomer (solid lines) and the photostationary state (dotted lines) of BTF6 (a) and DAMBTF6 (b) in chloroform. Fluorescence spectra of BTF6 (solid line) and DAMBTF6 (dashed line) are shown in (c).

Molecular conformations and their relative populations may have a profound effect on the chemical reactions and dynamics in liquids.[11] The dynamics of the ring closure reaction of diarylethene derivatives appears very complicated because the open isomer can have two conformations: the two aryl groups are oriented as either parallel (C_s symmetry) or antiparallel (C_2 symmetry) geometries.[3,12] The closed isomer has C_2 symmetry exclusively as long as it is prepared by the photoreaction of the open isomer. Because a molecule in C_2 symmetry is in a favorable geometry for the ring closure reaction via conrotatory mode, the C_2 conformer can easily undergo the ring closure reaction, whereas the C_s cannot.[13]

Dynamics of both the ring closure and opening reactions have been studied. The photochromic ring opening reaction was reported to occur in the region of a hundred picoseconds.[2,14−17] Previous studies on the photochromic ring closure reaction of diarylethene derivatives have shown that the reaction takes place in the picosecond time scale, although their dynamics are quite complicated.[15,18−27] Tamai et al. reported that in the case of diarylethene with thiophene oliogmer, the intermediate species are formed within 100 fs, followed by the closed isomer formation in 1.1 ps.[23] Kryschi and co-workers reported that a precursor state is formed in 1 ps followed by the ring closure in less than 10 ps for 1,2-bis(2-methylthien-3-yl)perfluorocyclopentene.[15,21] For 1,2-bis(5-phenyl-2-methylthien-3-yl)cyclopentene, Hania et al. suggested a preswitching dynamics of rapid mixing and relaxation of the electronic states occurring on the subpicosecond time scale followed by the ring closure in 4.2 ps.[22,28] Ring closure of around 3 ps was also reported for bis-(5-pyridyl-2-methylthien-3-yl)perfluorocyclopentene.[19] Interestingly, Miyasaka et al. reported that the ring closure reaction of 2-bis(2,4,5-trimethyl-3-thienyl)maleic anhydride proceeds in two pathways: a fast process occurring in 1−2 ps and a slow pathway occurring in several hundred picoseconds, where the latter is solvent viscosity dependent.[24]

Presumably, the complexity of the ring closure mechanism is considerably attributable to the conformational diversity of the open isomer. The intrinsic ambiguity of the transient absorption (TA) method is also partly responsible for the complication, as TA is used in all previous studies of the femtosecond dynamics. Interpretation of a TA signal is not always straightforward because a TA signal consists of several contributions originated from the ground state, excited state, and all product state.[29,30] On the other hand, time-resolved spontaneous fluorescence (TRF) provides unambiguous information on the population dynamics of the excited state.[31] Therefore, TRF is an ideal tool for the study of the dynamics of a reaction occurring in the electronic excited state such as the one investigated here, although femtosecond TRF has not been employed in the study of the photochromic ring closure reaction dynamics of the diarylethene compounds. One of the reasons might be that the C_2 conformer is known to undergo ultrafast ring closure reaction but does not fluoresce significantly, whereas the C_s conformer does not undergo the photochromic reaction but fluoresces significantly.[32]

In this work, we have investigated the photochromic ring closure reaction dynamics of the diarylethene derivatives shown in Scheme 1 using femtosecond TRF, although it is known that the photoactive C_2 conformer does not fluoresce significantly. One of the advantages of the TRF is that a molecule that absorbs light strongly must emit strongly before it relaxes, even when the fluorescence quantum yield is very low, because of the linear relationship between the Einstein A (spontaneous emission) and B (absorption) coefficients. That is, the C_2 conformer must emit strongly before the reaction takes place as far as the time resolution of the TRF apparatus is high enough to resolve it, because the C_2 conformer absorbs strongly. In our previous work,[17] we have successfully used TRF of the closed isomer to reveal the dynamics of the ring opening reaction of 1,2-bis(2-methylbenzo[*b*]thiophen-3-yl)hexafluorocyclopentene (BTF6, **1**), although it is known that the closed isomer does not emit.

Experimental Section

Femtosecond Time-Resolved Fluorescence Apparatus. Femtosecond TRF was acquired by the fluorescence upconversion method. The laser system for the TRF has been described in detail previously.[17] Briefly, it consists of a femtosecond Ti:sapphire oscillator (Tsunami, Spectra Physics), a home-built multipass Ti:sapphire amplifier operating at 5 kHz, and a noncollinear optical parametric amplifier (NOPA).[33] The NOPA was pumped by the second harmonic of the amplified fundamental at 800 nm to produce 50 fs pulses tunable across the visible. The output of the NOPA around 620 nm was frequency doubled and served as the excitation pulses. The remainder of the 800 nm output was used as a gate in the fluorescence upconversion.

The TRF apparatus has been described in detail elsewhere.[34] The excitation pulse at around 310 nm was focused into a 200 μm path length flow cell by a 5 cm focal length lens. Fluorescence was collected and focused into an upconversion crystal by a reflective objective lens. The fluorescence and the 800 nm gate pulses were mixed in a 500 μm thick BBO crystal in a type I phase matching condition. Time resolution of the TRF apparatus was 150 fs (full width at half-maximum) as determined by the cross-correlation between the scattered pump and the gate pulses. Polarizations of the pump and the gate pulses were set to a magic angle to measure TRF signals independent of the polarization effects.

Picosecond TRF was measured by the time correlated single photon counting (TCSPC) method. In the TCSPC experiment, fluorescence was collected by a parabolic mirror, dispersed by a monochromator, and detected with a thermoelectrically cooled microchannel plate photomultiplier tube (Hamamatsu R3809U-51). Outputs of the photomultiplier tube (start pulse) and a fast photodiode (stop pulse) were processed by a pair of 1 GHz

amplifier/discriminator (EG&G Ortec, 9327) and analyzed by a picosecond time analyzer (EG&G Ortec, 9308). The width of the instrument response function was 50 ps.

Quantum Yield Measurement. Accurate measurement of the reaction quantum yield is important to substantiate the reaction mechanism. When products do not absorb the excitation light so that the reaction proceeds in forward direction only, a reaction quantum yield Q can be expressed by

$$QP(t) = -\frac{\mathrm{d}[R(t)]}{\mathrm{d}t} N_0 V \quad (1)$$

where $P(t)$ is the number of photons absorbed by the reactant per unit time at time t, $[R(t)]$ is the molar concentration of the reactant at time t, N_0 is the Avogadro's number, and V is the sample volume. Using Beer's law and integrating over t give

$$QP_0 \int_0^t [1 - T(t)]\,\mathrm{d}t = -(\epsilon \mathrm{b})^{-1} N_\mathrm{A} V[A(0) - A(t)] \quad (2)$$

where P_0 is the total number of photons per unit time, $T(t)$ is the transmittance at time t, ϵ is the molar extinction coefficient at the excitation wavelength, b is the path length of the cell, and $A(t)$ is the absorbance of the reactant at time t. Because the open isomer does not absorb in the visible, eq 2 can be used to obtain the quantum yield of the ring opening reaction by visible light, if the initial concentration of the closed isomer is known.

Because the ring opening as well as the ring closure can be initiated by the UV light, irradiation by the UV light creates a photostationary state where both the open and the closed isomers exist. In addition, both the open and closed isomers show comparable absorbance in the UV spectral region, as shown in Figure 1. Taking into account the ring opening reaction of the produced closed isomer by UV light during the measurement, eq 1 is modified to

$$\frac{\mathrm{d}[\mathrm{O}(t)]}{\mathrm{d}t} = -(N_\mathrm{A} V)^{-1}[P_0 Q^{\mathrm{closure}}(1 - 10^{-\epsilon_\mathrm{O} b[\mathrm{O}(t)]}) + P_0 Q^{\mathrm{opening}}(1 - 10^{-\epsilon_\mathrm{C} b[\mathrm{C}(t)]})] \quad (3)$$

with

$$A(t) = b\{\epsilon_\mathrm{O}[\mathrm{O}(t)] + \epsilon_\mathrm{C}[\mathrm{C}(t)]\}$$

$$[\mathrm{O}(0)] = [\mathrm{O}(t)] + [\mathrm{C}(t)]$$

where O and C represent the open and the closed isomers, respectively. At the photostationary state, $\mathrm{d}[\mathrm{O}(t)]/\mathrm{d}t = 0$ and the ratio of Q^{closure} and Q^{opening} at 310 nm can be obtained. Therefore, the ring closure reaction quantum yield can be obtained by measuring $[\mathrm{O}(t)]$.

The concentration of the open form in the photostationary state may be determined by NMR or another spectroscopic method afterward. Here, we measured the concentration of the open isomer directly from the fluorescence intensity of the solution. Because the absorption of the closed isomer at 310 nm is due to the S_n ($n \geq 2$) states and the S_1 band is centered at 550 nm, emission from the closed isomer is negligible in the 400∼480 nm region according to Kasha's rule.[35] Thus, the emission in the 400−480 nm region can be safely assigned to the open isomer. In addition, interconversion between the C_s and C_2 conformers is fast enough for the two conformers to be in equilibrium during the quantum yield measurement time scale, which is typically several seconds, although the interconversion rate is slow compared to the NMR time scale of 1 μs.[36]

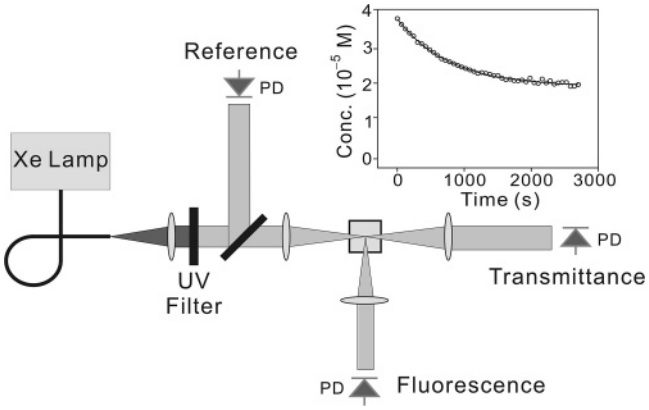

Figure 2. Schematic of the reaction quantum yield measurement setup. The inset shows a typical time trace of the emission intensity (converted to concentration) of **1O** vs exposure time of the 310 nm light.

The experimental setup for the quantum yield measurement is shown in Figure 2. A typical time trace of the fluorescence of the open isomer is also shown as an inset. A Xe lamp with a 10 nm bandpass filter centered at 310 nm and a frequency doubled Nd:YAG laser at 532 nm were used as excitation lights for the ring closure and opening reactions, respectively. Solutions of the open isomer with a known concentration of around 10^{-5} M in chloroform were prepared and stirred during the measurement. Intensities of the excitation and transmitted lights were monitored simultaneously by photodiodes. Fluorescence intensity was measured by a combination of a bandpass filter, a photodiode, and a lock-in amplifier. A beam splitter was placed in front of the sample to compensate for the intensity fluctuation of the excitation light sources. The power meter was calibrated and reflections from optical surfaces were also carefully compensated.

Materials and Sample Preparation. Molecular structures of 1,2-bis(2-methylbenzo[*b*]thiophen-3-yl)hexafluorocyclopentene (BTF6, **1**), 1,2-bis(6-acetyl-2-methylbenzo[*b*]thiophen-3-yl)hexafluorocyclopentene (DAMBTF6, **2**), and 1,2-bis(6-cyano-2-methylbenzo[*b*]thiophen-3-yl)hexafluorocyclopentene (DCYBTF6, **3**) in the open and closed configurations are shown in Scheme 1. Open isomers were synthesized according to the procedure reported previously.[37,38] The samples were dissolved in chloroform and flowed through a cell with a 200 μm path length to ensure fresh volume of sample on each shot during the measurement. The sample reservoir was irradiated by visible light during the TRF measurement to keep the molecules in open isomers and to avoid photoexcitation of the closed isomers of diarylethene derivatives by 310 nm light, which apparently induces photochemical degradation.

Results

Figure 1 shows the absorption and emission spectra of the open isomers and the photostationary states of compounds **1** and **2** at nearly the same concentrations. The absorption spectra of the photostationary states show a broad feature in the visible, which is the characteristic absorption band of the closed isomers.[1] Absorption bands **2O** (open isomer of **2**) and **2C** (closed isomer of **2**) are red-shifted from the corresponding isomers of **1** due to the substituted acetyl group. Emission maxima of **1O** and **2O** are observed at 430 and 450 nm, respectively. Note the large fluorescence intensity difference of the two compounds. In addition, the fluorescence quantum yield of **2O** is lower than that of **1O** by approximately 10 times, which agrees with the previous observation that an increase in

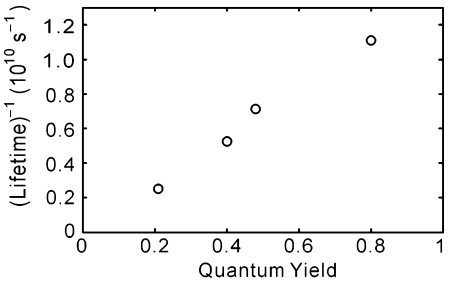

Figure 3. Decay rate of the slow component in the TRF vs reaction quantum yield for the diarylethene derivatives shown in Table 1.

TABLE 1: Decay Rate of the Slow Component in the TRF and the Reaction Quantum Yield for the Three Compounds Shown in Scheme 1 and 1,2-Bis(2-methylbenzo[b]thiophen-3-yl)maleic Anhydride (BTMA)

	quantum yield	lifetime (ps)
BTMA	0.21	400
DCYBTF6	0.40	190
BTF6	0.48	140
DAMBTF6	0.80	90

the ring closure reaction quantum yield (*vide infra*) leads to a decrease in the fluorescence intensity.[25]

A typical time trace of the fluorescence intensity of **1O** during the measurement of the ring closure quantum yield is shown in Figure 2. The system reaches the photostationary state at which the ring closure and opening reaction rates are equal. It can be seen that around 50% of the open isomer is converted to the closed isomer in the photostationary state. Because the concentration of the open isomer at time *t* can be obtained directly from the fluorescence intensity, the extinction coefficients of the open and the closed isomers at 310 nm can also be obtained from the absorbance. With these values, the ring closure reaction quantum yield can be obtained accurately by the integration of eq 3. The ring closure reaction quantum yields of **1O** and **2O** were calculated to be 0.48 and 0.80, respectively. Quantum yields of other compounds have also been measured and summarized in Table 1. The quantum yield of **1O** at 260 nm was reported to be 0.35 in hexane.[36] The quantum yield of the ring opening reaction of **1C** was measured to be 0.3, in close agreement with the previous report.[36]

Picosecond TRFs of the BTF6 derivatives were measured by the TCSPC method at their emission maxima. The emission originates from the open isomers in either C_2 or C_s conformations, and the decay reflects the weighted average of both conformers. The TRF of **1O** can be fitted well by a single exponential with a time constant of 150 ps, and that of **2O** decays double exponentially with ~4 and 90 ps time constants, where the 4 ps component is instrument-limited. The slow components for both compounds are much longer than the time scale of the ring closure reaction reported previously. Note that the 100 ps components were assigned to the population relaxation of the C_s conformer,[32] because the fluorescence of an open isomer was assigned to the C_s conformer that does not undergo the ring closure reaction. Picosecond TRFs of the other compounds were also measured and the results are listed in Table 1. Quite interestingly, the quantum yields and the decay rate ($1/\tau_{\text{lifetime}}$) show a linear relationship, as shown in Figure 3.

To time-resolve the ring closure reaction dynamics directly, femtosecond TRF was measured by the upconversion method. Figure 4 shows the normalized femtosecond TRF signals of **1O** at several detection wavelengths. Note that the TRF signal at 624 nm can be detected, although the stationary fluorescence intensity at $\lambda > 600$ nm is zero. The TRF signals can be fitted well by a two-exponential function with a fast component with ca. 1 ps time constant and a slow 100 ps component, as seen in the TCSPC measurements. The time constant of the fast component is similar to the values reported previously[15,19−24] and can be safely assigned to the direct ring closure reaction time. Interestingly, however, the relative amplitude and the time constant of the fast component show clear detection wavelength dependence: the time constant decreases and the relative amplitude increases as the detection wavelength increases. The time constants and relative amplitudes of the TRF of **1O** at several detection wavelengths are listed in Table 2. Note that the fast component is not observed for $\lambda < 450$ nm. Femtosecond TRF signals of **2O**, shown in Figure 5, are very similar to those of **1O**. The detection wavelength dependence is also the same, although the fast component is clearly observed at all detection wavelengths. The time constants and amplitudes of the TRF of **2O** are listed in Table 2.

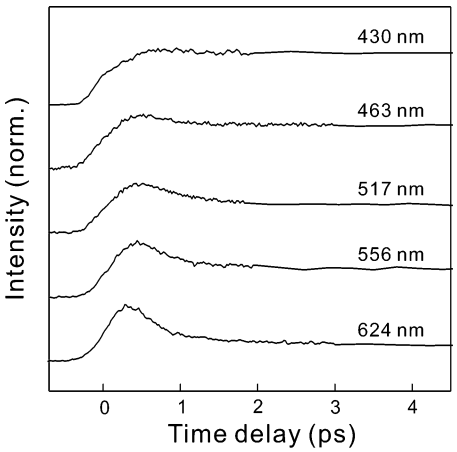

Figure 4. Representative TRF signals of BTF6 open isomer (**1O**) measured at several different wavelengths following the excitation at 310 nm.

TABLE 2: Fluorescence Decay Time Constants and Relative Amplitudes of BTF6 (1O) and DAMBTF6 (2O) at Various Detection Wavelengths[a]

1O			**2O**		
λ_{Det} (nm)	τ_1 (fs)	τ_2 (ps)	λ_{Det} (nm)	τ_1 (fs)	τ_2 (ps)
430		140 (1.0)	426	1700 (0.34)	89 (0.66)
446		150 (1.0)	447	1300 (0.38)	90 (0.62)
463	760 (0.40)	160 (0.60)	462	930 (0.47)	86 (0.53)
480	510 (0.68)	150 (0.32)	484	850 (0.52)	89 (0.48)
517	340 (0.78)	140 (0.22)	492	760 (0.56)	87 (0.44)
528	320 (0.92)	150 (0.08)	500	720 (0.62)	90 (0.38)
580	280 (0.97)	150 (0.03)	507	690 (0.63)	90 (0.37)
624	300 (0.98)	140 (0.02)	524	690 (0.69)	93 (0.31)

[a] Numbers in parentheses are the relative amplitudes.

Because the detection wavelength dependence indicates a change of the fluorescence spectrum in time, the TRF spectra were reconstructed from the TRF time traces at several detection wavelengths. Figure 6a shows the TRF spectra of **2O** at several time delays, compared with the stationary fluorescence spectrum. As implied from the TRF signals, the fluorescence spectrum shifts to blue rapidly and reaches the stationary state in a few picoseconds. To estimate the change of the average wavelength, the first moments of the spectra were calculated and shown in Figure 6b. The fluorescence shifts to blue by 3 nm in 900 fs. As expected, the time scale of the blue shift matches with the time scale of the fast decay component.

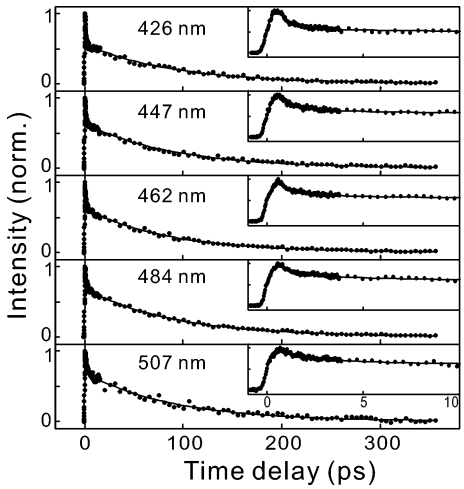

Figure 5. Representative TRF signals of DAMBTF6 open isomer (**2O**) measured at several different wavelengths following excitation at 315 nm. Insets show the signals in shorter time scale.

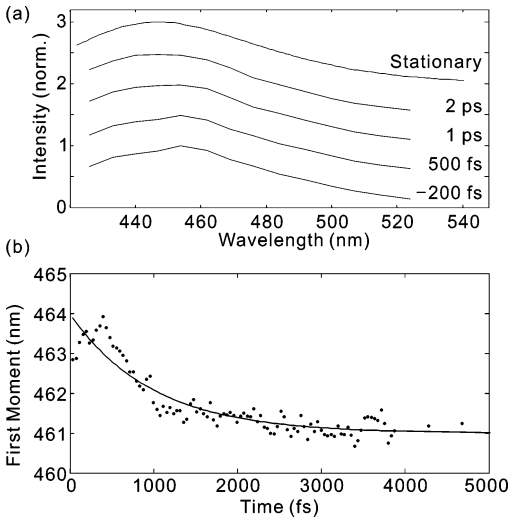

Figure 6. (a) TRF spectra of **2O** reconstructed from the time traces at several detection wavelengths. The stationary fluorescence spectrum is shown for comparison. (b) Average emission wavelength represented by the first moment of the spectra shown in (a). Note that the first moments do not match with the maxima of the TRF spectra due to the absence of the shorter wavelength region.

Discussion

We have investigated reaction dynamics of the photochromic diarylethene compounds by time-resolved fluorescence, which unambiguously measures the population of the excited chemical species. The TRF signals are relatively simple to show two exponential components with prominent detection wavelength dependence, although the TA spectra of the similar photochromic molecules reported previously are quite complicated. The TA spectra usually show bands over the entire UV/visible spectral region with several time constants.[15,22−24,28] Those were discussed in terms of preswitching dynamics[22] as well as intermediates. Because we have measured the decay of the reactants, not the formation of the products, we cannot rule out the possibility of the formation of intermediates. However, the TRF signals show instrument-limited rise and the spectra do not change significantly over time, indicating that the TRF signals originate from the same emitting species throughout the time window of this work. In addition, numerous transient absorption studies showed that the closed isomer is formed in a few picoseconds, the same time scale observed in this work; that is, the fast decay component in the TRF is due to the ring closure reaction directly from the initially excited state.

Populations of the C_s and C_2 conformers in liquids affect the reaction quantum yield and the dynamics profoundly. The relative populations of the C_s and C_2 conformers of **1O** in $CDCl_3$ are 35:65 when measured by NMR.[36] The rate of interconversion between C_s and C_2 should be slower than 1 μs, because they were observed as separate peaks in the NMR spectrum, but fast enough to be in equilibrium in solution during the quantum yield measurement time scale. Quantum mechanical calculations also found that the C_2 conformer is the major component in most of the related compound.[36,39−41] A related compound, 1,2-bis-(2-methyl-5-(2-(4-benzoylphen-1-yl)ethen-1-yl)thien-3-yl)perfluorocyclopentene, shows C_s and C_2 populations of 12:88 in a semiempirical calculation.[15] Quantum yields above 0.5 were observed for several diarylethene molecules to confirm that that the relative population of the C_2 conformer is higher than 0.5.[1,42] The high ring closure reaction quantum yield of **2O** also indicates that C_2 is the major conformer in the liquid and that it absorbs light strongly as well. These considerations establish that the fluorescence at initial times must be due to the open isomer that reacts.

The TRF signals show two time constants of around 1 and 100 ps, where the fast time constant can be assigned to the ring closure reaction time. It was suggested that fluorescence of the dithienylethene compounds in the open form originates from the C_s conformer that does not undergo the ring closure reaction.[32] Thus, it is tempting to assign the slow component to the C_s conformer. However, the fact that the C_2 conformer is the major component in the liquid and that the reaction quantum yield is much higher than 0.5 in **2O** indicates that the C_2 conformer may also be responsible for the slow component. Moreover, the linear relationship between the fluorescence decay rate of the slow component and the ring closure quantum yield strongly suggests that the slow component is due to the C_2 conformer that reacts. That is, the slow reaction channel competes with the population relaxation to the ground state by the internal conversion, as their rates are comparable. The slow reaction channel may also compete with the conformational dynamics to the C_s conformer, if C_s is lower in energy than C_2 in the excited state.

Thus, the reaction proceeds by the two channels: fast ~1 ps and slow ~100 ps time scales. It should be noted that the two channels do not imply two parallel processes, although they both arise from the C_2 isomer; only one rate constant would be observed for a reaction with two parallel channels from a common kinetic intermediate. The conclusion is in line with the report by Miyasaka et al.,[24] where the solvent viscosity effect on the photochromic reaction rates of 2-bis(2,4,5-trimethyl-3-thienyl)maleic anhydride (TMTMA) was measured by femtosecond transient absorption. They observed a fast <10 ps and a slow several hundred picosecond components with the latter being viscosity dependent. They also observed that the reaction quantum yield and the decay rate of the slow component in the fluorescence and TA signals are inversely proportional to the solvent viscosity, which led to the conclusion that the reaction undergoes by two channels: a direct fast pathway in less than 10 ps and a slow pathway through conformational dynamics. One problem of this conclusion is that all TRF signals are attributed to the C_2 conformer, and the emission from the C_s conformer is absent. A possibility is that the radiative lifetime of the C_s conformer is much longer (that is, the oscillator strength is smaller) than that of the C_2 conformer to show negligible intensity in the TRF.[12]

The fast component in the TRF shows distinctive detection wavelength dependence: its relative amplitude increases and the time constant shortens at longer wavelengths. The short component is detected even at the wavelengths where the intensity of the stationary fluorescence spectra is zero. It is to be noted that the fast component is not due to the closed isomer, because the fluorescence lifetime of the closed isomer was reported to be 22 ps irrespective of the detection wavelength.[17] The reaction product, the closed isomer, is formed in the ground state through conical interaction, because we do not observe emission from the closed isomer all times, although the closed isomer does emit with the emission maximum around 630 nm with a 22 ps lifetime.[17] The detection wavelength dependence can be translated into the spectral dynamics as shown in Figure 6. Such fluorescence spectral dynamics in time can be originated from various relaxation processes of the excited state such as the solvation, vibrational relaxation, and conformational changes. Relaxation of the excited state in any circumstances, however, cannot reproduce the blue shift observed in this work, because the ground state is at the potential minimum in terms of the nuclear coordinates and the relaxation processes in the excited state are energy dissipation processes. We considered another possibility that the system consists of a distribution of spectroscopically distinct chemical species in the excited state and the species emitting in the red side exhibit shorter lifetimes than those emitting in the blue side. Specifically, we considered a possibility that the dihedral angles that distinguish the C_2 and C_s conformers are distributed over a broad range and those emitting in the red undergo the ring closure reaction faster than those emitting in the blue. In this model, the excitation of the open isomer in some conformation creates an excited state that emits in the red side and undergoes the ring closure reaction directly in around 1 ps through conical intersection,[26] whereas the excitation of some other conformers creates an excited state that emits in the blue side and undergoes the ring closure reaction slowly in about 100 ps via conformational change.

To examine the conformational inhomogeneity along the reaction coordinate, we have performed quantum mechanical calculations on the ground state using the density functional theory. Comprehensive *ab initio* calculations on the related compounds have been reported previously,[22,26,39,43] and here we focus only on the aspect of conformational flexibility. The calculation of BTF6 was carried out using the Gaussian 03 package with the B3LYP functional and the standard 6-31G* basis sets. Two stable geometries close to the C_2 and C_s conformers are obtained in the geometry optimization procedure. The energy difference between the two is 125 cm^{-1} to give a relative population (C_s:C_2) of 1:2, in good agreement with the previous results.[36] Next, we calculated the potential surface around the C_2 conformation along the two dihedral angles to determine the distribution, and the results are shown in Figure 7. In the figure the positive ($+\theta_1$, $+\theta_2$) diagonal direction corresponds to the conrotatory ring closure reaction coordinate. The cross section along the diagonal direction is shown in Figure 8. Interestingly, the potential surface along the diagonal direction is much shallower than the off-diagonal directions; that is, the molecules have a broad distribution of the dihedral angles along the reaction coordinate at room temperature. The vertical excitation energies for the open and closed forms of BTF6 are calculated to be 336 and 545 nm, respectively, which are in agreement with the experimental values. Figure 9 shows the calculated structures and the highest occupied molecular orbitals (HOMOs) of the ground and vertically excited states for both **1O** and **1C**. The ground-state HOMOs of **1O** and **1C** show the

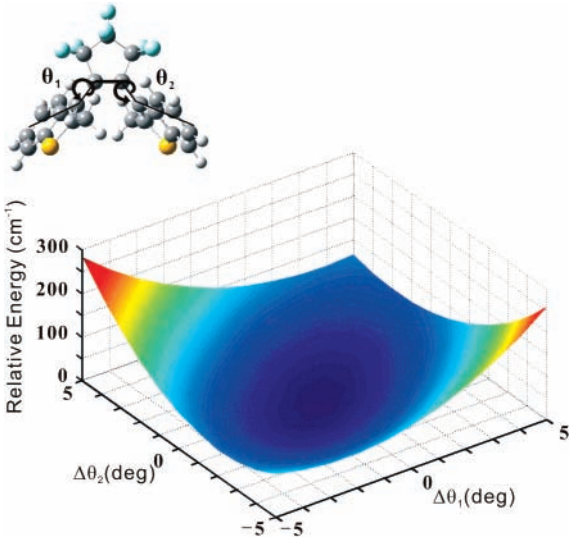

Figure 7. Potential energy surface of the ground state of **1O** in antiparallel (C_2) conformation along the two dihedral angles generated by the *ab initio* calculation.

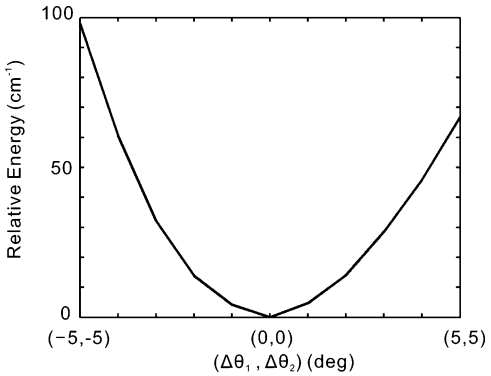

Figure 8. Cross section of the potential energy surface shown in Figure 8 along the ($+\theta_1$, $+\theta_2$) direction, which is the conrotatory reaction coordinate.

antibonding and bonding characters between the two adjacent sulfur atoms, respectively, whereas their corresponding excited-state HOMOs show bonding and antibonding characters, respectively. This explains how the electrons are excited and why the open form is closed and the closed form is opened by excitation.

Compiling all the theoretical and experimental results such as the stationary absorption and emission spectra, bimodal TRF decays, and their wavelength dependences, the potential energy surfaces responsible for the photochromic reaction dynamics of **1O** are proposed in Figure 10. Previous results on the ring opening reaction dynamics by TRF of the closed isomer are also considered, where a considerable barrier for the ring opening reaction was indicated. In Figure 10, two potential minima emitting at 420 and ~600 nm, which are responsible for the slow and fast fluorescence decays, respectively, are indicated. According to the picture, initial excitation and subsequent ultrafast vibronic and electronic relaxations create at least two states different in the conformation, from the broad conformational distribution of the molecules in the ground state. The one emitting in the long wavelength side undergoes fast direct ring closure reaction, perhaps through the conical interaction, whereas the one emitting in the short wavelength side undergoes conformational change prior to the ring closure. In our model, the red emitting species with a very large Stokes shift must lie closer to the product conformation than the blue

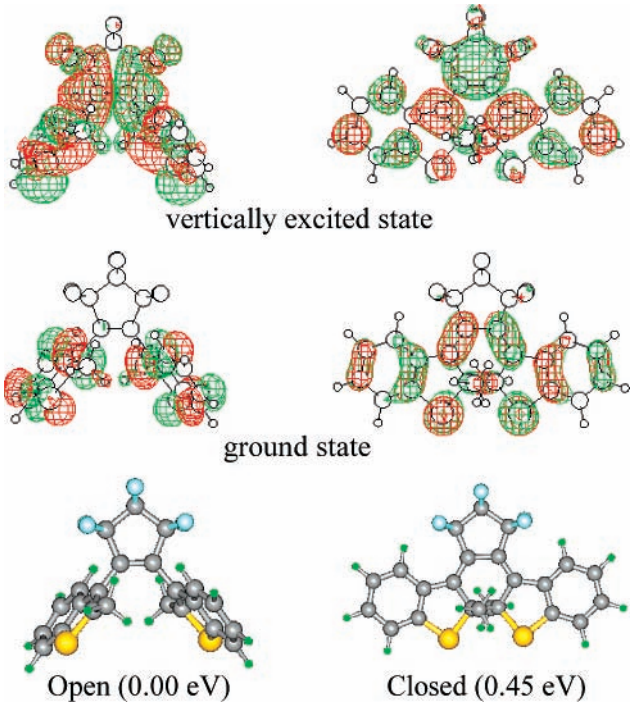

Figure 9. Structures and the ground- and vertically-excited-state HOMOs for both the open and closed forms of BTF6. Relative energies are given in eV.

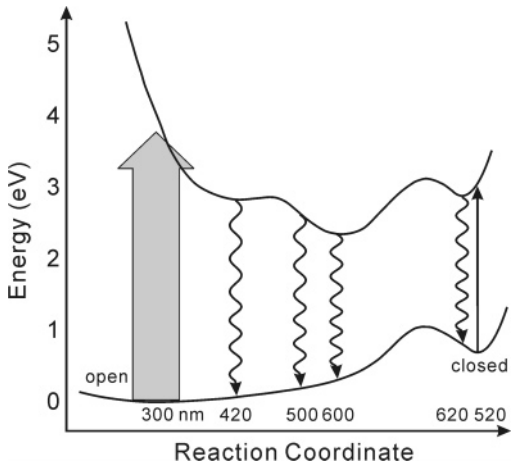

Figure 10. Schematic representation of the potential energy surfaces of BTF6 derivatives exhibiting photochromic reaction.

emitting species with a regular Stokes shift to undergo ultrafast reaction. This is possible when the ground-state potential surface along the reaction coordinate is rather flat and the excited-state potential surface decreases steeply toward the product. The potential energy curves reported by Hania et al. show a sign of such behavior to corroborate our model, when the potential energy curves are calculated and optimized in the excited state.[22]

The slow 100 ps component was assigned to the ring closure reaction through the conformational dynamics, which is controlled by the solvation dynamics in the liquid. The reaction dynamics may show multiexponential behavior, because the solvation dynamics is usually described by a series of time scales ranging from 100 fs to nanoseconds.[30,44] The solvation dynamics of the chloroform, however, shows only two time constants of 285 fs and 4.15 ps,[44] much shorter than the reaction time scale. In this diffusion-limited barrier crossing, the reaction can be well described by a single rate constant to give single exponential behavior.

Although qualitative features are the same for **1O** and **2O**, they are different in one important respect: **1O** does not show the fast decay component in the TRF at wavelengths shorter than the stationary fluorescence maximum. Contrary to the previous reports,[15,18−27] this suggests that the slow channel is the major path to the closed isomer for **1O**; that is, the ring closure reaction in **1O** occurs mostly via the slow conformational change. This also suggest that the two potential minima for **1O** are more clearly separated than in **2O**, which may account for the relatively low reaction quantum yield of **1O**. For **2O**, the short component occurs at all wavelengths with significant amplitudes, although the slow channel is still the major path, as shown in Table 2. Thus, the strategies to increase the reaction quantum yield should be 2-fold: to increase the population of the C_2 conformation and to open up the fast channel by controlling the conformation of the open isomer.

Conclusions

We have measured femtosecond time-resolved spontaneous fluorescence of the open isomer in the photochromic reaction of diarylethene derivatives. High time resolution and the advantages of the TRF facilitated the analysis of the complicated ring closure reaction dynamics. A fast decay component around 1 ps in the TRF of the open isomer was detected, whose amplitude and the time constant are detection wavelength dependent. Two emitting states were resolved: one emitting at the stationary fluorescence wavelength and the other emitting in the red side of the stationary fluorescence. The former undergoes slow ring closure reaction in ∼100 ps via conformational change, whereas the latter emitting in the red undergoes fast ring closure reaction in ∼1 ps possibly through the conical intersection. We suggest that initial broad distribution of the conformations around the dihedral angles of the two aromatic rings produce such distinct excited-state conformations.

Acknowledgment. This work was supported by the Korea Research Foundation Grant funded by the Korean Government (KRF-2004-005-C00007) and in part by POSTECH Core Research Program.

References and Notes

(1) Irie, M. *Chem. Rev.* **2000**, *100*, 1685−1716.
(2) Tamai, N.; Miyasaka, H. *Chem. Rev.* **2000**, *100*, 1875−1890.
(3) Hanazawa, M.; Sumiya, R.; Horikawa, Y.; Irie, M. *J. Chem. Soc., Chem. Commun.* **1992**, 206−207.
(4) Irie, M.; Eriguchi, T.; Takada, T.; Uchida, K. *Tetrahedron* **1997**, *53*, 12263−12271.
(5) Irie, M.; Lifka, T.; Uchida, K.; Kobatake, S.; Shindo, Y. *Chem. Commun.* **1999**, 747−748.
(6) Irie, S.; Yamaguchi, T.; Nakazumi, H.; Kobatake, S.; Irie, M. *Bull. Chem. Soc. Jpn.* **1999**, *72*, 1139−1142.
(7) Jeong, Y. C.; Park, D. G.; Kim, E.; Ahn, K. H.; Yang, S. I. *Chem. Commun.* **2006**, 1881−1883.
(8) de Jong, J. J. D.; Lucas, L. N.; Hania, R.; Pugzlys, A.; Kellogg, R. M.; Feringa, B. L.; Duppen, K.; van Esch, J. H. *Eur. J. Org. Chem.* **2003**, 1887−1893.
(9) Woodward, R. B.; Hoffman, R. *The Conservation of Orbital Symmetry*; Verlag Chemie: Weinheim, 1970.
(10) Atkins, P.; Friedman, R. *Molecular Quantum Mechanics*, 4th ed.; Oxford University Press: Oxford, U.K., 2005.
(11) Ziolek, M.; Kubicki, J.; Maciejewski, A.; Naskrecki, R.; Luniewski, W.; Grabowska, A. *J. Photochem. Photobiol. A−Chem.* **2006**, *180*, 101−108.
(12) Irie, M.; Sayo, K. *J. Phys. Chem.* **1992**, *96*, 7671−7674.
(13) Irie, M.; Miyatake, O.; Uchida, K. *J. Am. Chem. Soc.* **1992**, *114*, 8715−8716.
(14) Miyasaka, H.; Araki, S.; Tabata, A.; Nobuto, T.; Mataga, N.; Irie, M. *Chem. Phys. Lett.* **1994**, *230*, 249−254.
(15) Ern, J.; Bens, A. T.; Martin, H. D.; Kuldova, K.; Trommsdorff, H. P.; Kryschi, C. *J. Phys. Chem. A* **2002**, *106*, 1654−1660.
(16) Ern, J.; Bens, A. T.; Martin, H. D.; Mukamel, S.; Schmid, D.; Tretiak, S.; Tsiper, E.; Kryschi, C. *Chem. Phys.* **1999**, *246*, 115−125.

(17) Shim, S. D.; Joo, T.; Bae, S. C.; Kim, K. S.; Kim, E. Y. *J. Phys. Chem. A* **2003**, *107*, 8106−8110.

(18) Gentili, P. L.; Danilov, E.; Ortica, F.; Rodgers, M. A. J.; Favaro, G. *Photochem. Photobiol. Sci.* **2004**, *3*, 886−891.

(19) Owrutsky, J. C.; Nelson, H. H.; Baronavski, A. P.; Kim, O. K.; Tsivgoulis, G. M.; Gilat, S. L.; Lehn, J. M. *Chem. Phys. Lett.* **1998**, *293*, 555−563.

(20) Rini, M.; Holm, A. K.; Nibbering, E. T. J.; Fidder, H. *J. Am. Chem. Soc.* **2003**, *125*, 3028−3034.

(21) Ern, J.; Bens, A.; Martin, H. D.; Mukamel, S.; Schmid, D.; Tretiak, S.; Tsiper, E.; Kryschi, C. *J. Lumin.* **2000**, *87*−*89*, 742−744.

(22) Hania, P. R.; Telesca, R.; Lucas, L. N.; Pugzlys, A.; van Esch, J.; Feringa, B. L.; Snijders, J. G.; Duppen, K. *J. Phys. Chem. A* **2002**, *106*, 8498−8507.

(23) Tamai, N.; Saika, T.; Shimidzu, T.; Irie, M. *J. Phys. Chem.* **1996**, *100*, 4689−4692.

(24) Miyasaka, H.; Nobuto, T.; Murakami, M.; Itaya, A.; Tamai, N.; Irie, M. *J. Phys. Chem. A* **2002**, *106*, 8096−8102.

(25) Yagi, K.; Soong, C. F.; Irie, M. *J. Org. Chem.* **2001**, *66*, 5419−5423.

(26) Tamura, H.; Nanbu, S.; Ishida, T.; Nakamura, H. *J. Chem. Phys.* **2006**, *124*, 084313.

(27) Okabe, C.; Nakabayashi, T.; Nishi, N.; Fukaminato, T.; Kawai, T.; Irie, M.; Sekiya, H. *J. Phys. Chem. A* **2003**, *107*, 5384−5390.

(28) Hania, P. R.; Pugzlys, A.; Lucas, L. N.; de Jong, J. J. D.; Feringa, B. L.; van Esch, J. H.; Jonkman, H. T.; Duppen, K. *J. Phys. Chem. A* **2005**, *109*, 9437−9442.

(29) Mukamel, S. *Principles of Nonlinear Optical Spectroscopy*; Oxford University Press: Oxford, U.K., 1995.

(30) Joo, T.; Jia, Y. W.; Yu, J. Y.; Lang, M. J.; Fleming, G. R. *J. Chem. Phys.* **1996**, *104*, 6089−6108.

(31) Rhee, H.; Joo, T.; Aratani, N.; Osuka, A.; Cho, S.; Kim, D. *J. Chem. Phys.* **2006**, *125*, 074902−074901−074908.

(32) Ern, J.; Bens, A. T.; Martin, H. D.; Mukamel, S.; Tretiak, S.; Tsyganenko, K.; Kuldova, K.; Trommsdorff, H. P.; Kryschi, C. *J. Phys. Chem. A* **2001**, *105*, 1741−1749.

(33) Wilhelm, T.; Piel, J.; Riedle, E. *Opt. Lett.* **1997**, *22*, 1494−1496.

(34) Rhee, H.; Joo, T. *Opt. Lett.* **2005**, *30*, 96−98.

(35) Kasha, M. *Discuss. Faraday. Soc.* **1950**, *9*, 14−18.

(36) Uchida, K.; Tsuchida, E.; Aoi, Y.; Nakamura, S.; Irie, M. *Chem. Lett.* **1999**, 63−64.

(37) Irie, M.; Miyatake, O.; Uchida, K.; Eriguchi, T. *J. Am. Chem. Soc.* **1994**, *116*, 9894−9900.

(38) Kim, E.; Choi, Y.-K.; Lee, M.-H. *Macromolecules* **1999**, *32*, 4855−4860.

(39) Majumdar, D.; Lee, H. M.; Kim, J.; Kim, K. S.; Mhin, B. J. *J. Chem. Phys.* **1999**, *111*, 5866−5872.

(40) Okabe, C.; Tanaka, N.; Fukaminato, T.; Kawai, T.; Irie, M.; Nibu, Y.; Shimada, H.; Goldberg, A.; Nakamura, S.; Sekiya, H. *Chem. Phys. Lett.* **2002**, *357*, 113−118.

(41) Uchida, K.; Guillaumont, D.; Tsuchida, E.; Mochizuki, G.; Irie, M.; Murakami, A.; Nakamura, S. *J. Mol. Struct.* (*THEOCHEM)* **2002**, *579*, 115−120.

(42) Matsuda, K.; Shinkai, Y.; Yamaguchi, T.; Nomiyama, K.; Isayama, M.; Irie, M. *Chem. Lett.* **2003**, *32*, 1178−1179.

(43) Guillaumont, D.; Kobayashi, T.; Kanda, K.; Miyasaka, H.; Uchida, K.; Kobatake, S.; Shibata, K.; Nakamura, S.; Irie, M. *J. Phys. Chem. A* **2002**, *106*, 7222−7227.

(44) Horng, M. L.; Gardecki, J. A.; Papazyan, A.; Maroncelli, M. *J. Phys. Chem.* **1995**, *99*, 17311−17337.